Male accessory sex organ morphogenesis is altered by loss of function of Hoxd-13

Podlasek, Carol A.; Duboule, Denis; Bushman, Wade

DEVELOPMENTAL DYNAMICS 208:454–465 (1997)

Male Accessory Sex Organ Morphogenesis Is Altered by Loss of Function of Hoxd-13

CAROL A. PODLASEK,[1] DENIS DUBOULE,[2] AND WADE BUSHMAN[1]*
[1]*Urology Department, Northwestern University Medical School, Chicago, Illinois*
[2]*Department of Zoology and Animal Biology, University of Geneva, Sciences III, 1211 Geneva 4, Switzerland*

ABSTRACT **The role of the Hox gene Hoxd-13 in postnatal morphogenesis of the male accessory sex organs was examined by correlating the distribution and temporal regulation of expression in the accessory sex organs of postnatal mice with morphologic abnormalities of Hoxd-13-deficient transgenic mice. Previous studies of Hoxd-13 expression in the perinatal period have shown a broad domain of expression in the lower genitourinary tract, with expression in both mesenchyme and epithelium; focal expression was also noted in the epithelium of the nascent ducts of the developing prostate. Quantitative RT-PCR studies of Hoxd-13 expression in the 5 day mouse confirm widespread expression in the accessory sex organs developing from both the Wolffian duct and the urogenital sinus. Expression is downregulated with age, and a detailed time course of expression in the developing prostate shows that the level of Hoxd-13 expression correlates with morphogenetic activity in the development of the prostate ductal system. Transgenic Hoxd-13-deficient mice display multiple abnormalities in the male accessory sex organs. The most severe abnormalities were observed in organs exhibiting ductal branching during postnatal development and included diminished mesenchymal folding in the seminal vesicles, decreased size and diminished ductal branching in the ventral and dorsal prostate, and agenesis of the bulbourethral gland. We conclude that Hoxd-13 expression in the postnatal period correlates with a period of intense morphogenetic activity in accessory sex organ development and that the function of Hoxd-13 is evidenced by morphologic abnormalities in accessory sex organs of the Hoxd-13-deficient mutant.** ***Dev. Dyn. 208:454–465, 1997.***

Key words: prostate; Hoxd-13; mutant; morphogenesis

INTRODUCTION

The accessory sex organs of the mouse are a series of ducts and glands contributing secretions to the ejaculate. They include the seminal vesicles and ampullary gland, which derive from the caudal Wollfian duct, and the coagulating gland, dorsal and ventral prostate, and bulbourethral gland, which derive from the urogenital sinus (Cunha and Lung, 1979; Cunha et al., 1992). Formation of these individual structures is induced in late gestation in response to testosterone stimulation and involves both inductive and instructive interactions between epithelium and mesenchyme (Cunha et al., 1992); however, the organs are rudimentary at birth, and morphogenesis of these structures occurs largely in the postnatal period. Postnatal development is androgen dependent, and recent work has implicated fibroblast growth factor 7 (FGF-7; Sugimura et al., 1993) and transforming growth factor-β (TGF-β; C. Lee, personal communication) as mediators of mesenchymal-epithelial signaling, but the molecular mechanisms regulating morphogenesis remain poorly understood. We present here the first evidence that Hox gene expression is necessary for normal accessory sex organ development.

The murine Hox genes are a family of 39 homeobox-containing genes arranged in four chromosomal clusters (Scott, 1992), which share organizational and sequence homologies, are expressed in similar patterns during development (Morgan and Tabin, 1994; Dolle et al., 1991a), and provide a large degree of functional redundancy. Within each cluster (A, B, C, or D) the genes are expressed sequentially according to their 3′–5′ position. This produces a characteristic pattern of expression in which 5′ genes are expressed later and more posteriorly (or distally) along a developmental axis (Krumlauf, 1994; Dolle and Duboule, 1989; Dolle et al., 1989; Izpisua-Belmonte et al., 1991). In the developing limb, gut, and vertebral column, Hox gene expression is associated with patterning and segmentation events in early development and, subsequently, with growth and morphogenesis of specific structures (Izpisua-Belmonte and Duboule, 1992; Roberts et al., 1995; Hayamizu et al., 1994; Nelson et al., 1996). The functional significance of these associations has been proved in the limb and vertebral column by morphologic abnormalities induced by changes in patterns of Hox expression. Mice with an engineered loss of expression of a specific Hox gene may exhibit abnormalities that reflect changes in segmental patterning (homeotic

*Correspondence to: Wade Bushman, Urology Department, Northwestern University, Tarry Building 11-715, 303 E. Chicago Ave., Chicago, IL 60611.
Received 11 September 1996; Accepted 18 December 1996

transformation) or dysmorphic growth (agenesis or hypomorphism; Rijli et al., 1995; Duboule, 1994; Benson et al., 1995).

The genitourinary tract can be considered a developmental axis that undergoes segmental patterning and subsequent region-specific morphogenetic growth. Function of Hox genes in genitourinary development was first suggested by characteristic colinear patterns of Hox gene expression in the genitourinary tract during late gestation (Dolle et al., 1991a). The function of the Hox genes in patterning of genitourinary development was demonstrated by homeotic transformations in the epididymis-ductus deferens of the male (Hsieh-Li et al., 1995) and oviduct-uterus of the female (Benson et al., 1996) in transgenic mutants of Hoxa-11 and Hoxa-10, respectively. Hoxd-13 is the most 5′ member of the Hox D cluster. It is expressed in the developing limb and in a broad domain in the posterior body axis, including the tail, hindgut, and genital tubercle (Dolle et al., 1991a,b). Expression in the developing urogenital tract is abundant during late gestation and continues into the postnatal period (Oefelein et al., 1996).

We report here that quantitative analysis of Hoxd-13 expression in the seminal vesicle and prostate reveals a unique time course of expression in each structure that correlates with the distinctive patterns of postnatal morphogenesis. Examination of Hoxd-13-deficient animals reveals genitourinary abnormalities, including bulbourethral gland agenesis and abnormal seminal vesicle and prostate morphogenesis, showing that Hoxd-13 is required for normal accessory sex organ development.

RESULTS

Postnatal Expression of Hoxd-13

Among the Hox D cluster genes expressed in the urogenital tract of the late-gestation embryo, the domain of Hoxd-13 expression is the most caudal (Dolle et al., 1991a). Previous studies of prenatal expression by in situ hybridization revealed expression in both mesenchyme and epithelium of the Wolffian duct and urogenital sinus (Oefelein et al., 1996). Expression in both tissue layers has been confirmed by RT-PCR of mesenchyme and epithelium isolated from the 15 day embryo urogenital sinus (unpublished observation). The domain of expression of Hoxd-13 postnatally was found to include expression localized to the nascent ducts of the developing prostate, suggesting a role for Hoxd-13 in postnatal ductal morphogenesis (Oefelein et al., 1996). A quantitative method of RT-PCR was developed and used to examine Hoxd-13 expression in the lower genitourinary tract organs in the early postnatal period. All of the lower genitourinary tract tissues of 5-day-old mice showed Hoxd-13 expression. Expression was highest in the seminal vesicle and lowest in the testes and bulbourethral gland, but expression varied only fourfold across this range (Fig. 1). By comparison, there was not significant expression in the 5 day heart (data not shown). These data confirm a broad domain of Hoxd-13 expression in the lower genitourinary tract during the early postnatal period.

Correlation of Hoxd-13 Expression With Postnatal Morphogenesis

The pattern of postnatal morphogenesis is unique in each of the sex accessory sex organs. It has been most intensively studied and best characterized in the (dorsal and ventral) prostate and seminal vesicles. The prostate gland is an exocrine gland comprising a complex branched ductal network connected to the proximal urethra. The dorsal and ventral lobes are distinguished by unique architecture and histology of the ductal system, but both arise from multiple epithelial buds from the urogenital sinus, which grow into and branch within the surrounding urogenital sinus mesenchyme. Ductal budding begins at approximately 16 days of gestation and continues up to 10 days postnatally. Branching morphogenesis of the prostate ducts begins prenatally, is most intense during the first 2 weeks of life, and tapers gradually until prostate development is completed at approximately 60 days of age (Sugimura et al., 1986a). Morphogenesis of the seminal vesicles displays a different time course. At birth, the seminal vesicle is a simple, epithelium-lined, cane-like tube surrounded by mesenchyme. Epithelial branching morphogenesis of seminal vesicles, which is echoed by clefting of the surrounding mesenchyme, begins on day 2 or 3 postnatally, with intense growth and branching morphogenesis apparent during the first week postnatally (Cunha and Lung, 1979). Quantitative RT-PCR was used to examine quantitatively the expression in the prostate and seminal vesicles after birth, in order to determine whether decreasing expression postnatally (Oefelein et al., 1996) occurs as a simple function of time or is related to completion of morphogenesis.

Hoxd-13 expression in the prostate was highest in the newborn and decreased sixfold from birth to adulthood (Fig. 2). The gradual and progressive decrease in expression parallels the time course of prostate ductal morphogenesis shown by previous quantitative morphologic analysis (Sugimura et al., 1986a). Hoxd-13 expression is also highest in the newborn seminal vesicles (Fig. 3) and shows a progressive decrease of similar magnitude, but the time course is distinctly different. The abrupt decrease in expression after the first week contrasts with the pattern of expression in the prostate and correlates with a shorter time course of branching morphogenesis in the seminal vesicle.

Segmental Distribution of Hoxd-13 Expression in the Prostate Ducts

Morphogenesis of the prostate ductal network occurs by a process of concentrated mitotic activity at the duct tips and duct elongation and branching (Sugimura et al., 1986a,b). Localization of expression by in situ hybridization beyond 5 days postnatally was not pos-

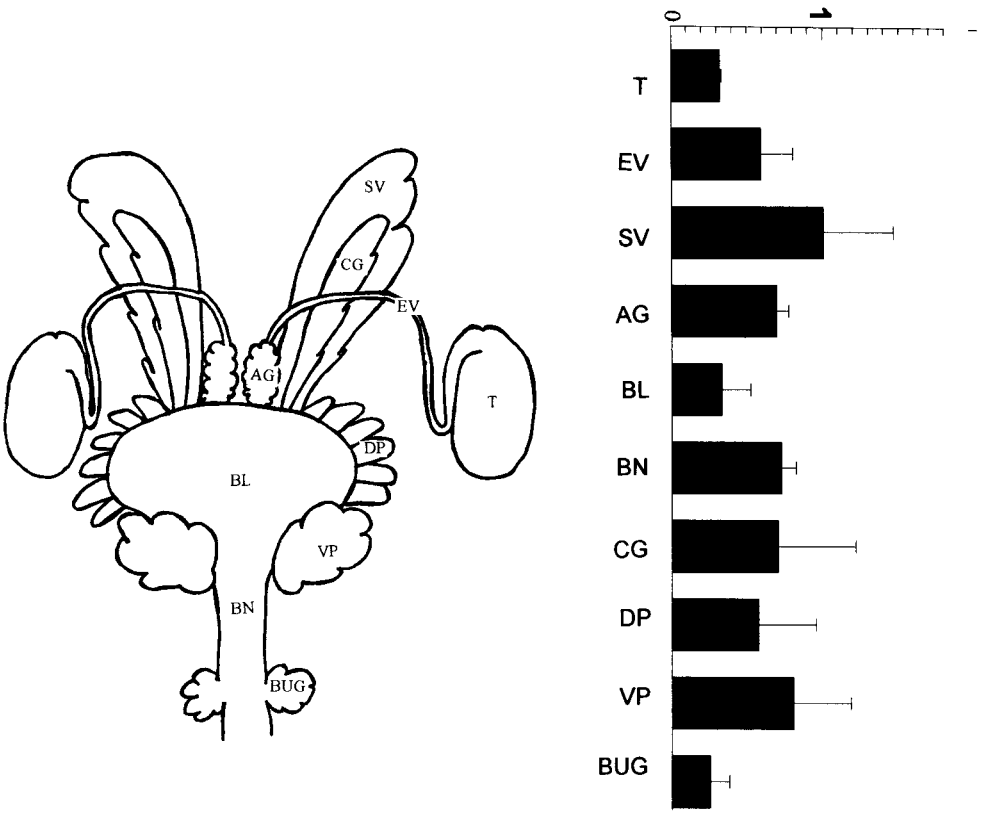

Fig. 1. **Left:** Schematic diagram of the lower genitourinary tract structures, showing testes (T); Wolffian duct derivatives, including epididymis/vas deferens (EV), ampullary gland (AG), and seminal vesicle (SV); and urogenital sinus derivatives, including bladder (BL), coagulating gland (CG), dorsal prostate (DP), ventral prostate (VP), bladder neck (BN), and bulbourethral gland (BUG). To facilitate comparison of expression in the different tissues, the data have been normalized so that the seminal vesicle expression is equal to one. **Right:** Relative level of expression of Hoxd-13 in the lower tract structures of the 5 day male. Hoxd-13 expression was quantitated for each tissue relative to expression of the ribosomal subunit RPL19 as described in the text and normalized to expression in the seminal vesicles.

sible because of diminished signal (Oefelein et al., 1996), so we used quantitative RT-PCR to compare the distribution of expression in the different regions of the ductal system of adolescent (13 day) mice. The ductal architecture of the ventral and dorsal prostate lobes was microdissected and divided into three parts: proximal duct segments (closest to the urethra), middle segments (containing many branch points and some duct tips), and distal segments (containing mostly duct tips). In both lobes, expression was approximately twofold higher in the proximal segments than in the distal segments; expression in the middle segments was intermediate (data not shown). For comparison, we examined the expression in the ductal system of adult mice in which homeostatic mitotic activity is also localized to the duct tips (Sugimura et al., 1986a). A twofold difference was again observed favoring the proximal segments in both the dorsal and the ventral lobes (data not shown). A twofold difference by quantitative RT-PCR is of borderline significance. However, the consistency of the observation in both lobes at both ages suggests that it is real and clearly argues against a correlation of expression with mitotic activity in the duct tips (Sugimura et al., 1986b).

Effect of Loss of Expression of Hoxd-13 on Accessory Sex Organ Morphogenesis

The functional association of Hoxd-13 with postnatal morphogenesis was tested by examining accessory sex organ morphology in transgenic mice deficient for Hoxd-13. Eight adult Hoxd-13-deficient transgenic mice and five control mice of comparable age and weight were examined individually, blinded, and in random order to determine how loss of Hoxd-13 expression affected accessory sex organ development. The testes of mutant mice were equal in size and weight to those of controls. Histologic examination confirmed spermatogenesis and mature sperm production. The epididymis, ductus deferens, and bladder were normal in gross appearance and on histologic analysis. The remainder of the lower genitourinary tract, including the Wolffian duct derivatives (seminal vesicles and ampullary gland) and the urogenital sinus derivatives (coagulating gland, dorsal and ventral prostate, urethra, and bulbourethral gland), exhibited a spectrum of abnormalities (Table 1).

Wolffian duct derivatives. The Wolffian duct arises from the duct of the pronephros when this duct becomes associated with the developing mesonephros (Cunha

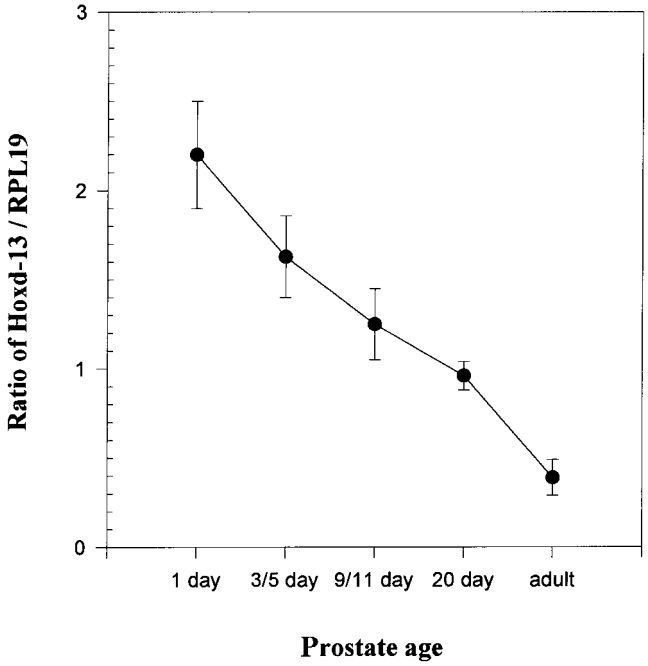

Fig. 2. Hoxd-13 expression in the developing prostate was analyzed by quantitative RT-PCR, which showed a progressive, sixfold decrease in expression between birth and adulthood. Expression is most abundant during the period of intense prostate ductal morphogenesis (days 1–20 postnatally). The absolute ratio of Hoxd-13 to RPL 19 product is presented.

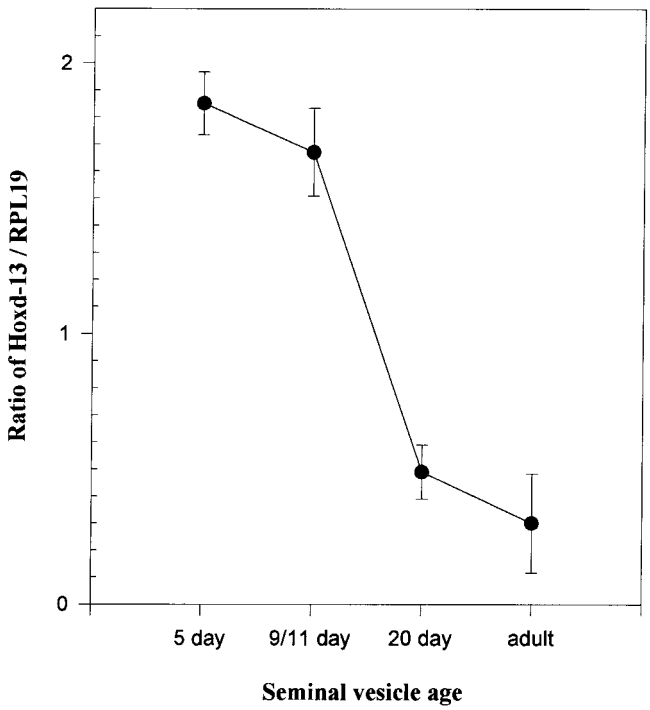

Fig. 3. Hoxd-13 expression in the seminal vesicle decreases sixfold between birth and adulthood. The temporal pattern of down-regulation in the seminal vesicles differs from that of the prostate and may reflect a unique time course of postnatal morphogenesis. The absolute ratio of Hoxd-13 to RPL 19 is presented.

and Lung, 1979). The onset of fetal androgens prevents programmed cell death of the Wolffian duct and stimulates development, including formation of the seminal vesicles and ampullary gland from the caudal end.

Seminal vesicles. The normal adult organ is characterized by a highly convoluted stromal sheath containing a secretory epithelium. The seminal vesicles of the mutant were of normal length and width; however, the number and depth of the folds in the stromal sheath were reduced (Fig. 4). The phenotype varied in severity but was clearly present in all animals examined. Additional defects were seen in two of eight animals examined. One animal had an ectopic kidney located in the contralateral pelvis. The seminal vesicle ipsilateral to the two kidneys was severely hypoplastic. In another animal, one seminal vesicle was massively dilated, suggesting the presence of ejaculatory duct obstruction. All mutant animals had normally colored (white) secretory material within the glands, and histologic examination revealed normal stromal and epithelial differentiation (not shown).

Ampullary gland. The ampullary gland comprises a cluster of secretory ducts surrounding the insertion of the ductus deferens in the urethra. This gland was minimally affected. Its size appeared to be slightly reduced, an effect that might result from shortened lengths of the ducts that make up the gland (Fig. 5). Histologic sections revealed normal epithelial and stromal differentiation (not shown).

Urogenital sinus derivatives. The urogenital sinus arises from the ventral aspect of the cloaca (Cunha and Lung, 1979). Testosterone induces the urogenital sinus to form the dorsal and ventral prostate, coagulating gland, and bulbourethral gland. These structures are connected to the proximal urethra (dorsal/ventral prostate and coagulating gland) or more distal urethral (bulbourethral gland) by one or more main ducts.

Coagulating gland. The coagulating gland consists of an interior layer of glandular epithelial cells surrounded by smooth muscle and a connective tissue sheath (Brandes and Portela, 1960). Each lobe consists of two or three main ducts, with a large number of secondary branch outgrowths from the main duct. The coagulating gland of the mutant was normal in size, but its appearance suggested a failure to attain the fully branched state of the normal adult. The ductal branches appeared to be shorter (Fig. 4, arrowheads), and there was increased thickness of the central (unbranched) mesenchyme (Fig. 4, asterisks). To quantitate the differences between the mutant and normal, the coagulating glands were microdissected and the number of duct tips was counted. Surprisingly, there was no apparent difference in the number of duct tips between the mutant and control (Fig. 6).

Dorsal prostate. The dorsal prostate in the mutant was reduced in size (Fig. 5). Whereas the dorsal prostate lobe is generally fanned out along the posterior

TABLE 1. Summary of Mutant Phenotypes

Tissue	Gross appearance	Histology
Ampullary gland	Decreased overall size, decreased length of ductal branches	Normal
Bladder neck and urethral glands	Increased diameter of the bladder neck/urethra	Dysmorphic urethral glandular elements
Bulbourethral gland	Absent in half of mutants, variable decrease in size in remainder	Normal
Coagulating gland	Decreased extent of ductal branch growth	Normal
Dorsal prostate	Decreased overall size, fewer main ducts	Normal
Ventral prostate	Decreased overall size but normal number of main ducts, total duct length is shorter, with increased number of short terminal branches	Normal
Seminal vesicles	Decreased glandular folding	Normal

margin of the proximal urethra, the dorsal prostate in the mutant occupied a smaller segment of this region. To determine whether quantifiable changes in branching morphogenesis of the prostate ductal system contribute to the reduced size, the dorsal prostates of mutant and control animals were microdissected to reveal the ductal architecture. The ductal network of the dorsal prostate normally develops from approximately 16 main ducts, arrayed along a broad base on the proximal urethra; the mutant had fewer main ducts (varying between 4 and 16) whose origins were restricted to a smaller area on the proximal urethra (Fig. 5). The extent of branching morphogenesis was quantitated by counting the number of ductal tips (Fig. 6). Comparison of mutant and controls revealed a 37% decrease in the number of duct tips in the mutant. This difference is statistically significant ($P = 0.0002$).

Ventral prostate. The ventral prostate also appeared to be reduced in size in the mutant (Fig. 5). The number of main ducts (two to six) was unchanged. Quantitative microdissection revealed a 15% decrease in the number of duct tips, but the difference was not statistically significant (Fig. 6). The major change in this lobe appeared to be in the pattern of ductal branching and the resulting architecture of the ductal system. The overall lengths of the ducts were diminished, and branch points were shifted from a more proximal location toward the duct tip (Fig. 7). Together these changes produced a gland that is smaller than would be expected on the basis of the decrease in duct tips alone. The histologic appearance of the ventral and dorsal prostate was normal (data not shown).

Proximal urethra. The proximal segment of the urethra (or bladder neck) is the site of entry of the main ducts of several accessory sex organs (the seminal vesicles, coagulating gland, and dorsal and ventral prostate), and it is normally lined by the urethral glands, mucus glands located in the submucosa. The diameter of the proximal urethra in the mutant appeared to be marginally increased. Histologic examination revealed a dysmorphic appearance of the submucosal glands at the level that is the site of entry of the main prostate ducts. The regular cellular arrangement of the glands was distorted and interspersed with disorganized glandular structures that resemble isolated ductal elements. Whereas the glandular elements are normally contained within a surrounding collar of smooth muscle, in the mutant the glands occasionally penetrated into the muscle layer (Fig. 8).

Bulbourethral gland. A unique and unexpected phenotype was observed in the bulbourethral gland, a branched mucus gland attached to the urethra. This gland was completely absent in half of the eight mutant animals examined. No vestigial remnant was observed. In the remaining animals, the gland was normal in appearance although usually somewhat reduced in size (Fig. 4). Ductal branching could not be quantitated in the bulbourethral gland, because its fragility precluded microdissection of the ductal tree. The histology of the gland, when it was present in the mutant, was normal.

DISCUSSION

Postnatal expression of Hoxd-13 in the lower genitourinary tract and morphologic abnormalities accompanying loss of function in transgenic mice implicate Hoxd-13 as a necessary factor in normal accessory sex organ development. Hox genes influence segmental patterning and postsegmentation morphogenesis in developmental systems such as the axial skeleton and limb. Hox genes also regulate segmental patterning of soft tissue systems, as shown by several recent observations (Hsieh-Li et al., 1995; Benson et al., 1996). However, the issue of whether Hox expression influences postsegmentation morphogenesis of soft tissues hinges upon correlating expression with later developmental events and evaluating the morphologic effects of changes in expression. The lower genitourinary tract is an attractive system in which to study Hox genes insofar as the structures are highly segmented and the components have unique and readily identifiable morphologic characteristics. Many of the structures undergo complex morphogenetic processes, such as ductal branching, which have been extensively studied and quantitatively described. Tissue development occurs primarily in the postnatal period, allowing quantitative measurement of gene expression by RT-PCR. We have quantitatively described the distribution and temporal regulation of Hoxd-13 expression during postnatal morphogenesis, correlated expression with the morphogen-

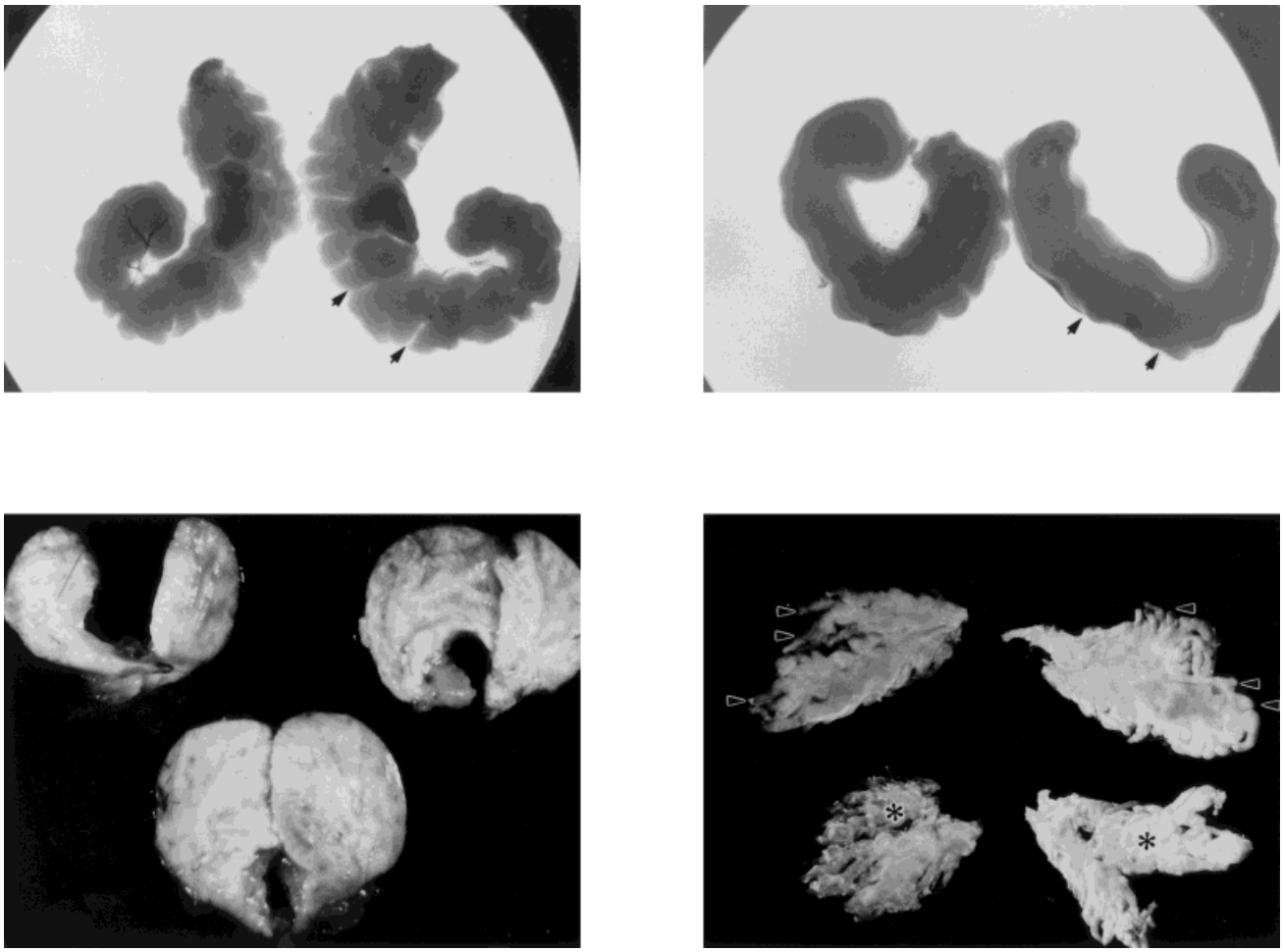

Fig. 4. Comparison of seminal vesicles from normal (**top left**) and mutant (**top right**) animals shows decreased folding (mesenchymal clefting, indicated by arrows) in the mutant. The bulbourethral gland showed two different types of abnormalities. In half of the mutants examined, no bulbourethral gland could be identified; when present, the gland was variably reduced in size. **Bottom left** panel compares two mutants (top) and one normal animal (bottom). Comparison of coagulating glands in the **bottom right** panel from normal (left) and mutant (right) animals shows decreased branching growth in the mutant (arrows) and an increase in the thickness of the central, unbranched mesenchyme (asterisks).

esis process, and systematically described the morphologic consequences of loss of expression.

Mice deficient in Hoxd-13 function showed diffuse morphologic changes in the accessory sex organs that echoed the broad domain of expression of Hoxd-13 normally present in the lower genitourinary tract during late gestation and postnatally. The mutant phenotype was clearly evident in branched structures, including the seminal vesicles and prostate where Hoxd-13 expression correlated with glandular morphogenesis. However, relative levels of expression in the different organs were not predictive of phenotype severity (Fig. 1). Some structures such as the bladder displayed significant Hoxd-13 expression but appeared normal in the mutant. Whether the difference in phenotype severity reflects a specific role for Hoxd-13 in branching morphogenesis, variable degrees of redundancy provided by paralogous genes, or simply a greater difficulty in detecting hypomorphic changes in unbranched structures such as the bladder remains undetermined.

Morphologic abnormalities in the seminal vesicles, coagulating gland, and prostate suggest that Hoxd-13 affects multiple facets of postnatal morphogenesis. The decreased number of main ducts in the dorsal prostate of the mutant together with the dysmorphic appearance of the proximal urethra at the site from which these ducts emerge suggests that expression of Hoxd-13 interferes with normal budding of the urogenital sinus to form the main ducts of the dorsal prostate. Decreased branching in the ventral prostate and diminished size of the ductal complex suggest that Hoxd-13 regulates ductal growth. Finally, diminished clefting of the seminal vesicle mesenchyme and increased thickness of central mesenchyme in the coagulating gland suggest deficient remodelling of the mesenchyme during postnatal development.

Work with the developing limb has suggested that Hox expression during morphogenesis may be linked to control of cell proliferation and growth (Duboule, 1994). However, we were unable to demonstrate colocalization

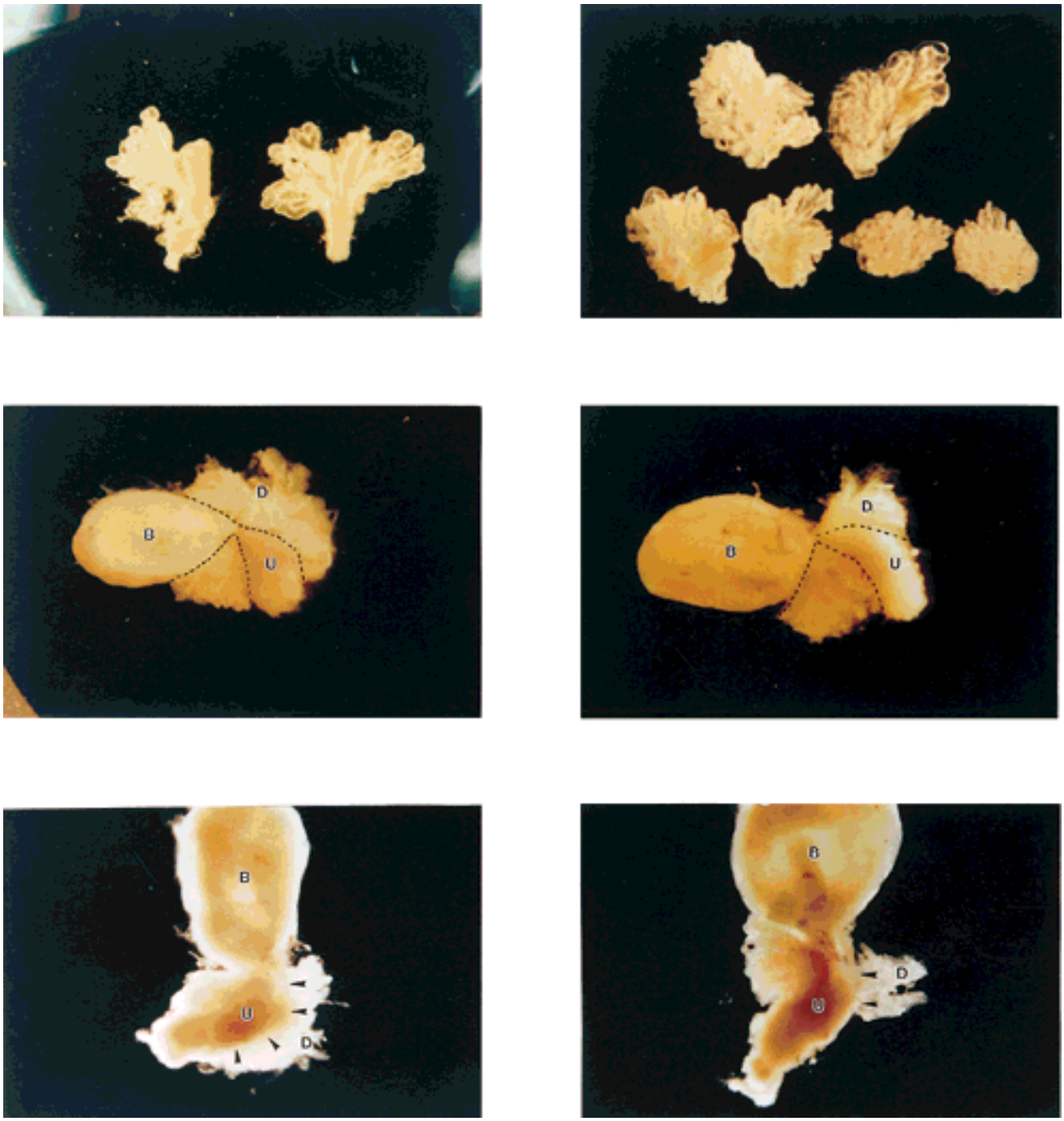

Fig. 5. **Top left:** Comparison of normal (left) and mutant (right) ampullary gland. **Top right:** Comparison of normal (top) and two mutant (bottom) ventral prostate, showing decreased size in the mutant ventral prostates. **Middle:** Comparison of normal adult (**left**) and mutant (**right**) bladder neck region. Dashed lines outline the base of the dorsal prostate superior to and the urethra. Note decreased dorsal prostate size in the mutant and a narrower point of origin from the urethra. The ventral prostate inferior to the urethra is also outlined for clarity. **Bottom:** Comparison of same region from 30 day normal (**left**) and mutant (**right**) animals clearly shows a broad base of dorsal prostate ductal development from the urethra in the normal animal (arrowheads) vs. a more restricted point of origin in the mutant. B, bladder; D, dorsal prostate; U, urethra.

of expression with the known distribution of mitotic activity within the ductal system of the adolescent and adult prostate. In fact, expression was consistently twofold higher in the proximal duct segments shown by labelling studies to be relatively mitotically quiescent (Sugimura et al., 1986b). The characteristics of the

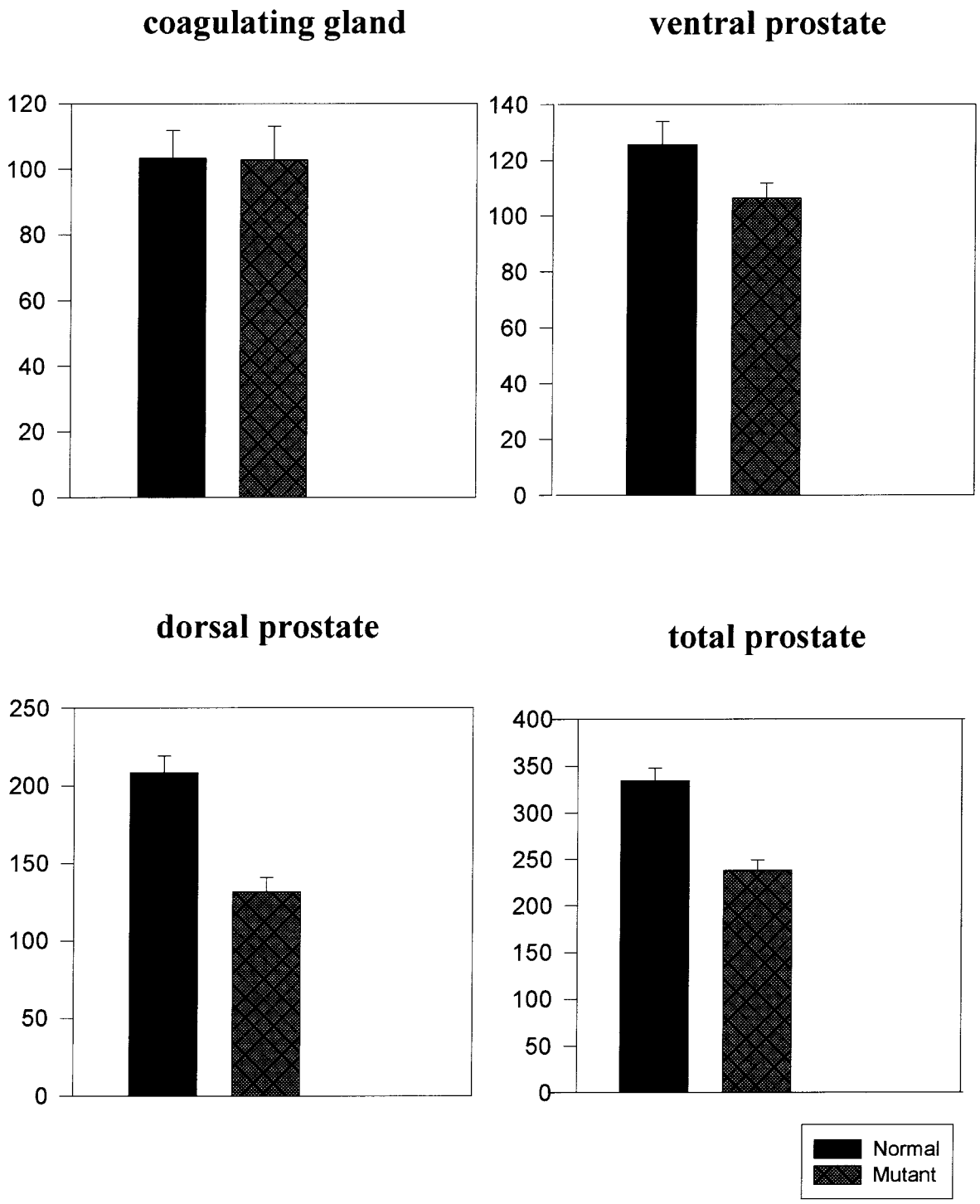

Fig. 6. Quantitative microdissection was performed to determine the number of ductal branch tips in the prostate lobes of normal and mutant animals. A comparison of coagulating gland duct tips in five controls and six mutants revealed no significant difference. A comparison of dorsal prostate and ventral prostate duct tips in five controls and eight mutants revealed a 37% decrease in duct tips in the dorsal prostate ($P = .0002$) and a 15% decrease in duct tips in the ventral prostate ($P = .07$). The number of duct tips in the total prostate (ventral prostate plus dorsal prostate) was reduced by 29% ($P = .0002$).

ductal system in the prostate are regionalized along the proximal-distal axis. The distal ducts (tips) are characterized by relatively high mitotic activity, androgen dependence, and scant periductal stroma composed largely of fibroblasts. The proximal segments are the site of apoptosis, display androgen independence, and are surrounded by a stroma rich in smooth muscle (Nemeth and Lee, 1996). The nonuniform distribution

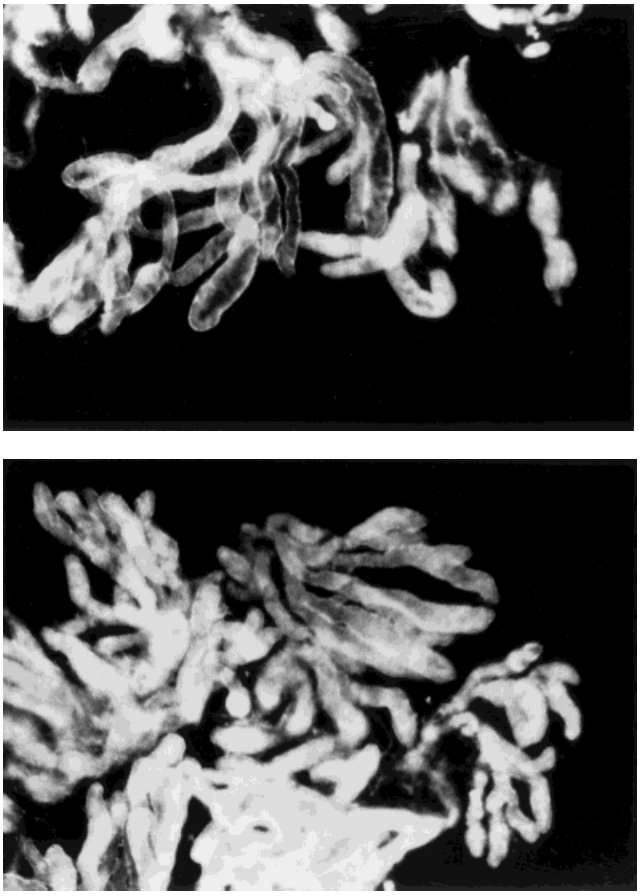

Fig. 7. Sample microdissection of the ventral prostate from normal (**top**) and mutant (**bottom**) animals showing a shortened overall duct length and increased number of short terminal branches in the mutant.

of Hoxd-13 expression along the duct axis raises the intriguing possibility that expression in this context may be connected to establishing and maintaining the proximal-distal regionalization of the prostatic ducts.

The single most striking abnormality of the genitourinary tract in the mutant mice was the absence of the bulbourethral gland in half of the animals examined. This could be interpreted as a severe form of hypomorphism; however, we would then expect a range of moderate to severe hypomorphism in the remaining animals. In fact, we observed only a moderate to mild degree of hypomorphism of the bulbourethral gland when present, comparable to effects seen in other structures, such as the seminal vesicles. The apparent discontinuity in the severity of the bulbourethral gland phenotype could reflect the operation of two different mechanisms, one affecting patterning in the prenatal period (in which loss of expression results in agenesis with variable penetrance) and another affecting postnatal morphogenesis and growth.

Our observations indicate that Hoxd-13 may play a significant role in prenatal patterning of soft tissues of the genitourinary tract and is necessary for postnatal accessory sex organ morphogenesis. These observations support the concept that highly conserved developmental mechanisms regulating development in other systems, such as the limb and gut, might also operate in the lower genitourinary tract and suggest novel approaches to investigating the induction and control of accessory sex organ development.

EXPERIMENTAL PROCEDURES

Animals

The production of mice deficient in Hoxd-13 function has been reported previously (Dolle et al., 1993). Expression studies for Hoxd-13 were performed on tissues from BalbC mice. Animals were housed and cared for in accordance with the NIH Guidelines for the Care and Use of Laboratory Animals. Specimens for RNA preparation were harvested from euthanized males. Through a midline incision, the entire genitourinary tract, including kidneys, ureters, bladder, seminal vesicles, ampullary gland, coagulating gland, testes, epididymis, ductus deferens, prostate complex, bulbourethral gland, and urethra, were isolated. The individual organs were identified and dissected using ×30 zoom magnification and sharp dissection and were snap frozen in liquid nitrogen.

Tissue Dissection

The morphologic sequences of deletion of Hoxd-13 expression were determined by examining animals +/+, +/−, and −/− for Hoxd-13 on a genetically equivalent background of mixed SV129 and C57 black. Animal genotyping was based on morphology of limbs and parent genotypes.

Morphologic analysis of the Hoxd-13 mutant (eight animals) and control (five animals) animals was performed by a blinded observer after the genitourinary tracts were isolated. The kidneys, testes, and epididymis were examined and then removed from the remaining genitourinary complex by division of the ductus deferens and ureters. Adipose and connective tissues surrounding the accessory sex organs were gently removed by a combination of sharp and blunt dissection such that the accessory sex organs could be inspected and photographed. The seminal vesicle, coagulating gland, ampullary gland, dorsal prostate, ventral prostate, and bulbourethral glands were isolated at their connections to the bladder neck and urethra. The individual organs were then quantitatively microdissected, photographed, and/or fixed in Bouin's solution or formalin for subsequent histologic examination. Microdissection of the ventral prostate and dorsal prostate glands was performed as previously described using collagenase to facilitate the process of microdissection (Sugimura et al., 1986b). The number of branch tips and main ducts was quantified in real time as the dissection was performed but was validated by subsequent examination of the photographed specimen. Quantitation of the ductal morphology in the coagulating gland and ampullary gland was performed in a similar fashion.

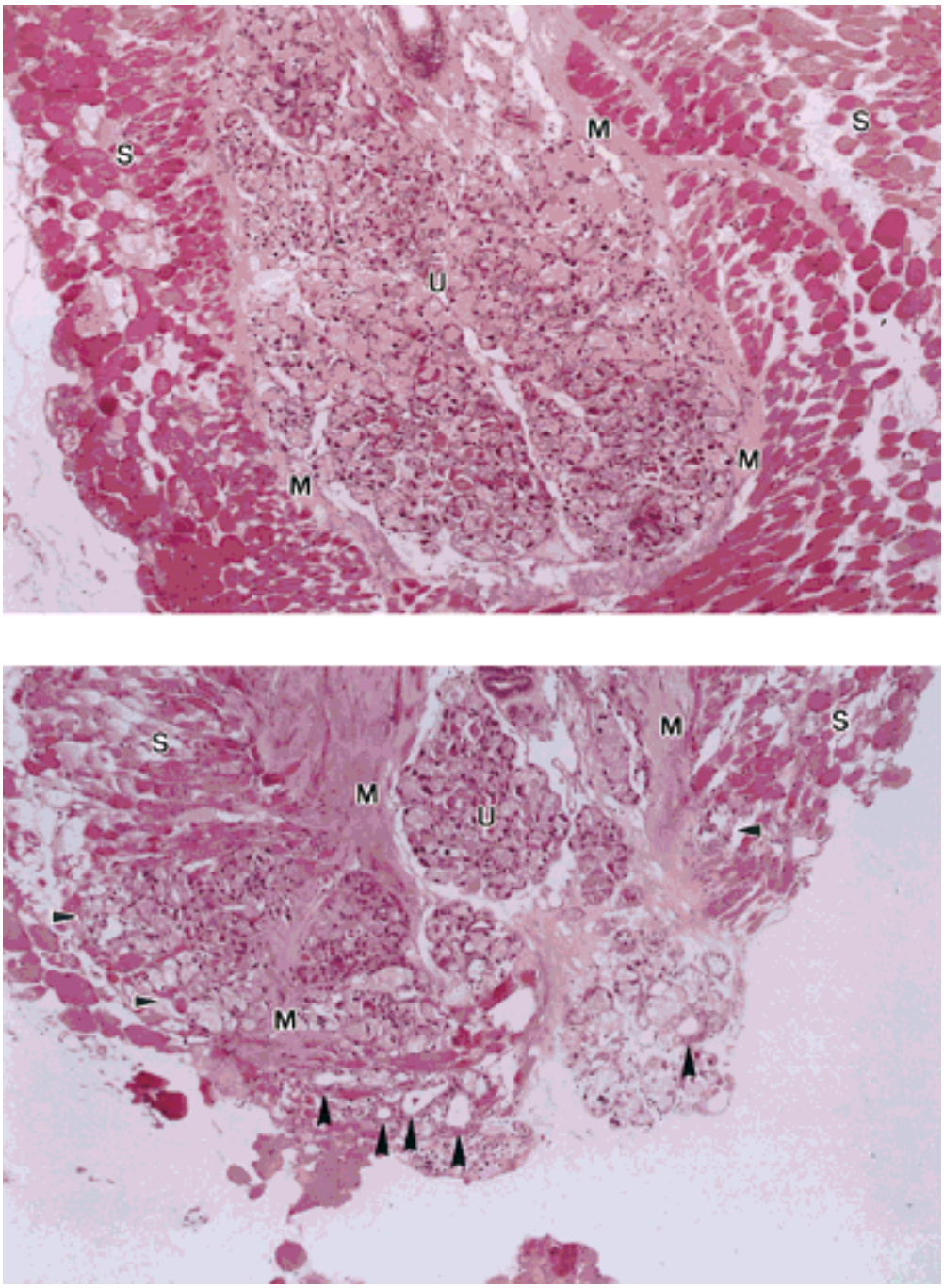

Fig. 8. Urethral glands (U) in the normal animal (**top**) are contained within a collar of smooth muscle (M) and separated by it from the surrounding striated muscle of the urethral sphincter (S). In the mutant animal (**bottom**), the glands penetrate the smooth muscle collar and invade the striated muscle (white-bordered arrowheads). Ductal structures with defined lumina, not normally seen within the urethral glands, are observed in the periphery of the glands (black arrowheads).

RNA Isolation

Total RNA from 5 day tissues was isolated from pooled specimens (n = 5) using a modified TRIzol procedure (Chomczynski, 1993; Chomczynski and Sacchi, 1987). Tissues were homogenized with a mortar and pestle and an 18 gauge syringe in TRIzol (1 ml/0.1 g) and were incubated for 5 min. Five day tissues had 27 µg of carrier tRNA (*E. coli* strain W, type XXI; Sigma,

St. Louis, MO) added for precipitation in the later steps. Chloroform (200 µl) was added and the mixture incubated at room temperature for 3 min. The mixture was centrifuged in an Eppendorf 5415C centrifuge at 14,000 rpm (all centrifugations were performed at this speed) for 15 min, to separate the phases. The aqueous layer was drawn off and the RNA precipitated overnight in an equal volume of isopropanol (−20°C). The RNA was centrifuged for 15 min and the pellet washed with 70% cold ethanol. The pellet was air dried and resuspended in 10 µl DEPC-treated water for each tissue homogenized (e.g., the RNA of five prostates was diluted with 50 µl DEPC-treated water).

DNase Treatment

All RNA was DNase treated as follows: 25 µg RNA, 10 µl 5× TSC buffer (Promega, Madison, WI), 78 units RNasin (Promega), 3 units DNase (Promega), and DEPC-treated water made up to 50 µl were incubated in a 37°C water bath for 30 min. Fifty microliters of DEPC-treated water and 100 µl phenol:chloroform (50:50) were added, and the mixture was centrifuged at 14,000 rpm for 10 min. The aqueous layer was added to 100 µl chloroform and the mixture was centrifuged for 5 minutes at 14,000 rpm. Eleven microliters of 3 M NaOAc (pH 5.2) and 220 µl 100% ethanol were added to the aqueous layer. The RNA was allowed to precipitate at −80°C for 2 hr and centrifuged for 15 min at 14,000 rpm. The pellet was washed with 70% ethanol, centrifuged for 10 min (14,000 rpm), air dried for 2 minutes, and resuspended in 10 µl DEPC-treated water.

Quantitative RT-PCR

RT-PCR was performed to examine Hoxd-13 relative to RPL19 (a gene coding for a ribosomal subunit protein) as an internal standard, using the Perkin Elmer RT-PCR kit. The primer sequences (5′ to 3′) of Hoxd-13 and RPL19 are as follows: Hoxd-13S, TTAAAC CAG CCG GAC ATG TG; Hoxd-13AS, GAC AGT GTC TTT GAG CTT GG; RPL19S, CTC AGG CTA CAG AAG AGG CTT; and RPL19AS, GGA CAG AGT CTT GAT GAT CTC. The Hoxd-13 and RPL19 primers yield 230 bp and 560 bp products, respectively. The RT step was performed in one tube containing 5 mM $MgCl_2$, 1× PCR buffer II, 1 mM of each nucleotide, 1 unit RNase inhibitor, 2.5 µM random hexamers, 2.5 units MuLV reverse transcriptase, and 3 µl total RNA (total volume 64 µl). This mixture was incubated at 42°C for 15 min, 99°C for 5 min, and 5°C for 5 min. PCR reagents (250 µl containing 2.5 units AmpliTaq, 2 mM $MgCl_2$, 1× 10× PCR buffer II, 0.4 µg sense and antisense primers of both Hoxd-13 and RPL19, and water) were added to the tube containing the RT mixture (314 µl). Five 45 µl aliquots were pipetted into PCR tubes, and PCR was performed as follows: incubation for 2 min at 95°C, 1 min at 95°C, 1 minute at 60°C, and 1 min at 72°C. A tube was removed at cycle numbers 20, 23, 26, 29, and 32, and 40 µl of each sample was electrophoresed on 1.2% agarose (Mallinckrodt; pulsed field GenAR agarose) gel containing 0.5 µg/ml ethidium bromide. Densitometry of the photographed gel was performed using a PDI densitometer. The area under each peak was determined by cutting out and weighing the peaks from the densitometer tracing. The log of band density vs. cycle number was plotted for both RPL19 and Hoxd-13 to find the linear range. For all reactions, 23 and 26 cycles were within the linear range. The average of the ratios of Hoxd13 to RPL19 at 23 and 26 cycles was considered the ratio of products within the linear range. This indirect method of quantitative RT-PCR was selected because the amount of RNA isolated from neonatal tissues precludes accurate quantitation by other methods. Comparisons of expression between samples of unknown starting RNA concentration are possible when performed in the linear range of PCR for the gene of interest and an internal standard (Seibert, 1993). Control experiments demonstrated that the Hoxd-13/RPL19 product ratio varied 2% over a 25-fold range and less than 25% over a 100-fold range of input RNA. The sample RNAs in all PCR experiments estimated on the basis of tissue weight as well as spectrophotometric measurement were centered within this 25-fold range. DNA contamination of RNA was excluded by performing RT-PCR for 35 cycles in the absence of reverse transcriptase.

ACKNOWLEDGMENTS

The authors thank Joska Zakany for his help, the Schweppe Foundation of Chicago (W.B.), the Edwin Beer Program of the New York Academy of Medicine (W.B.), the Swiss National Fund (D.D.), and the HFSBO (D.D.) for support.

REFERENCES

Benson, G.V., Nguyen, T.E., and Maas, R.L. (1995) The expression pattern of the murine Hoxa-10 gene and the sequence recognition of its homeodomain reveal specific properties of abdominal B-like genes. Mol. Cell. Biol. 15:1591–1601.

Benson, G.V., Lim, H., Paria, B.C., Satokata, I., Dey, S.K., and Maas, R.L. (1996) Mechanisms of reduced fertility in Hoxa-10 mutant mice: Uterine homeosis and loss of maternal Hoxa-10 epression. Development 122:2687–2696.

Brandes, D., and Portela, A. (1960) The fine structure of the epithelial cells of the mouse prostate. J. Biophys. Biochem. Cytol. 7:505–509.

Chomczynski, P. (1993) A reagent for the single-step simultaneous isolation of RNA, DNA and proteins from cell and tissue samples. Biotechniques 15:532.

Chomczynski, P., and Sacchi, N. (1987) Single-step method of RNA isolation by acid guanidinium thiocyanate-phenol-chloroform extraction. Anal. Biochem. 162:156.

Cunha, G.R., and Lung, B. (1979) Development of male accessory glands. In: "Accessory Glands of the Male Reproductive Tract." Ann Arbor, MI: Ann Arbor Science, Vol. 6, pp. 1–28.

Cunha, G.R., Alarid, E.T., Turner, T., Donjacour, A.A., Boutin, E.L., and Foster, B.A. (1992) Normal and abnormal development of the male urogenital trace. J. Androl. 13:465–475.

Dolle, P., and Duboule, D. (1989) The structural and functional organization of the murine Hox gene family resembles that of *Drosophila* homeotic genes. EMBO J. 8:1507–1515.

Dolle, P., Izpisua-Belmonte, J.-C., Falkenstein, H., Renucci, A., and Duboule, D. (1989) Coordinate expression of the murine Hox-5 complex homeobox-containing genes during limb pattern formation. Nature 342:767–772.

Dolle, P., Belmonte, I., Brown, J.M., Tickle, C., and Duboule, D. (1991a) Hox-4 genes and the morphogenesis of mammalian genitalia. Genes Dev. 5:1767–1776.

Dolle, P., Izpisua-Belmonte, J., Boncinelli, E., and Duboule, D. (1991b) The Hox-4.8 gene is localized at the 5′ extremity of the Hox-4 complex and is expressed in the most posterior parts of the body during development. Mech. Dev. 36:3–13.

Dolle, P., Dierich, A., LeMur, M., Schimmang, T., Schuhbaur, B., Chambon, P., and Duboule, D. (1993) Disruption of the Hoxd-13 gene induces localized heterochrony leading to mice with neotenic limbs. Cell 75:431–441.

Duboule, D. (1994) How to make a limb? Science 266:575–576.

Hayamizu, T.F., Wanek, N., Taylor, G., Trevino, C., Shi, C., Anderson, R., Gardiner, D.M., Muneoka, K., and Bryant, S. (1994) Regeneration of HoxD expression domains during pattern regulation in chick wing buds. Dev. Biol. 161:504–512.

Hsieh-Li, H.M., Witte, D.P., Weinstein, M., Branford, W., Li, H., and Small, K. (1995) Hoxa11 structure, extensive antisense transcription, and function in male and female fertility. Development 121: 1373–1385.

Izpisua-Belmonte, J.-C., and Duboule, D. (1992) Homeobox genes and pattern formation in the vertebrate limb. Dev. Biol. 152:26–36.

Izpisua-Belmonte, J.-C., Tickle, C., Dolle, P., Wolpert, L., and Duboule, D. (1991) Expression of the homeobox Hox-4 genes and the specification of position in chick wing development. Nature 350:585–589.

Krumlauf, R. (1994) Hox genes in vertebrate development. Cell 78:191.

Morgan, B.A., and Tabin, C. (1994) Hox genes and growth: Early and late roles in limb bud morphogenesis. Development Suppl., pp. 181–186.

Nelson, C.E., Morgan, B.A., Burke, A.C., Laufer, E., Di Mambro, E., Murtaugh, L.C., Gonzales, E., Tessarollo, L., Parada, L.F., and Tabin, C. (1996) Analysis of Hox gene expression in the chick limb-bud. Development 122:1449–1466.

Nemeth, J.A., and Lee, C. (1996) Prostatic ductal system in rats: Regional variation in stromal organization. Prostate 28:124–128.

Oefelein, M., Chin-Chance, C., and Bushman, W. (1996) Expression of the homeotic gene Hox-d13 in the developing and adult mouse prostate. J. Urol. 155:342–346.

Rijli, F.M., Matuas, R., Pellegrini, M., Dierich, A., Gruss, P., Dolle, P., and Chambon, P. (1995) Cryptorchidism and homeotic transformations of spinal nerves and vertebrae in Hoxa-10 mutant mice. Proc. Natl. Acad. Sci. USA 92:8185–8189.

Roberts, D.J., Johnson, R.L., Burke, A.C., Nelson, C.E., Morgan, B.A., and Tabin C. (1995) Sonic Hedgehog is an endodermal signal inducing BMP-4 and Hox gene during induction and regulation of the chick hindgut. Development 121:3136–3174.

Scott, M.P. (1992) Vertebrate homeobox gene nomenclature. Cell 71:551–553.

Seibert, P. (1993) "Quantitative RT-PCR." Clontech Methods and Applications Book 3. Palo Alto, CA: Clontech Laboratories.

Sugimura, Y., Cunha, G.R., and Donjacour, A.A. (1986a) Morphogenesis of ductal networks in the mouse prostate. Biol. Reprod. 34:961–970.

Sugimura, Y., Cunha, G.R., Donjacour, A.A., Bigsby, R.M., and Brody, J.R. (1986b) Whole-mount autoradiography study of DNA synthetic activity during postnatal development and androgen-induced regeneration in the mouse prostate. Biol. Reprod. 34:985–995.

Sugimura, Y., Cunha, G.R., Hayward, S., Haysahi, N., Arima, K., Kawamura, J., Rubin, J., and Aaronson, S. (1993) Keratinocyte growth factor (KGF) is a mediator of testosterone-induced prostatic development. Differ. Ther. 1:423.